

Effect of Hydrogen on the Microstructure Evolution of Nanocrystalline Silicon

Amita Sharma*

Author's Affiliations:

Amita Sharma Department of Physics, R.D.S. College, Muzaffarpur, 842001, Bihar India.
*Corresponding author: **Amita Sharma**, Department of Physics, R.D.S. College, Muzaffarpur, 842001, Bihar India.
E-mail: dramitasharma63@gmail.com

Received on 25.03.2019

Accepted on 02.05.2019

ABSTRACT We have studied the effect of hydrogen on the microstructure evolution of nanocrystalline silicon. We have performed molecular dynamics simulations to identify the role of hydrogen on the nanocrystalline silicon recrystallization phenomena. It requires an accurate description of any relevant atomic scale feature. We have taken advances in computer modeling of nanocrystalline silicon and the development of quantitative analysis tools. We have characterized the microstructure evolution of nanocrystalline silicon by varying both the crystallinity and the hydrogen content. We have estimated the rate of recrystallization as a function of the hydrogenation and showed that the boundary mobility decreased exponentially with hydrogen due to the occurrence of clustering and to the accumulation of the hydride at the boundaries. We have studied the atomistic details of the elementary recrystallization process investigating the ability of dissolved hydrogen to slow down the mobility of the amorphous crystalline boundaries. The effect is enhanced by increasing the hydrogen content with a recrystallization rate that decreased exponentially with hydrogen concentration. We found that at low concentration the hydrogen tended to migrate from the crystal phase to amorphous one directly affecting the thickness of the grain boundaries and increased their effective interface.

KEYWORDS Microstructure, nanocrystalline, hydrogenation, mobility, clustering, atomistic, amorphous, concentration.

INTRODUCTION

Vetterl et al. [1] studied the coexistence of nanocrystals and amorphous regions optimally combines the stability against light induced degradation and the electrical conductivity of the crystalline phase with the red-infrared optical absorption of the amorphous phase. Spinella et al. [2] and Cleri et al. [3] showed that nanocrystalline silicon is a complex material with a broad range of different microstructures that can form close to the amorphous to crystal phase transformation and whose properties largely depends on the actual intermixing of the two phases. Bergen et al. [4] and Voyles et al. [5] presented that the amount of crystalline phase X in nanocrystalline silicon crystalline systems formed by randomly oriented nanocrystals separated by thin grain boundaries down to $X \sim 0.2$ in systems where the more abundant amorphous phase embeds a dispersion of non aggregated nanocrystals such as spherical shaped nano grains paracrystalline silicon, elongated crystal fibers like textured silicon and many others. Lucovsky et al. [6] and Math et al. [7] showed that among several processing issues hydrogenation is critical in affecting the electronic properties of nanocrystalline-silicon. High quality films require hydrogen content around 10%. Tauc et al. [8] showed that hydrogen is inserted in order to passivate dangling bonds in the amorphous phase and to release

microscopic strain thus restoring a electronic energy gap and reducing the concentration of recombination centers. Zhang et al. [9] showed that above results enabled the applications of hydrogenated nanocrystalline silicon in optoelectronics and photovoltaics through an increased conductivity of photo excited carriers. Bagolini et al. [10] demonstrated that hydrogen affects the nature of the electronic localization in the a-silicon phase of nanocrystalline silicon samples and promoted quantum confinement effects. Codet et al. [11] and Shama et al. [12] indicated the importance of hydrogen in nanocrystalline silicon processed by plasma chemical vapor deposition since it can either promote the formation of nanovoids. Olson et al. [13] and Xu et al. [14] showed that when hydrogen is dispersed in the film, it affects the relative stability between the amorphous and the crystalline phases and in turn the mobility of the phase boundaries during the solid phase crystallization of nanocrystalline and hydrogen.

METHOD

We prepared a set of pure nanocrystalline silicon systems with different crystal to amorphous ratios. We quenched from the melt a periodically repeated silicon crystal slab formed by 2x50x50 cubic unit cells, each cell having lateral size of 0.54305 nm and contained eight atoms according to the equilibrium density of carbon silicon. The dimension of the system was $L_x=1.086\text{nm}$, $L_y=27.15\text{ nm}$ and $L_z=27.15\text{nm}$ and it contained 40,000 silicon atoms. Isolated grains was then inserted in the amorphous slaby following a twofold procedure, at first the grains were extracted from a perfect silicon lattice in such a way that their [100] crystallographic direction was parallel to the x- direction of the simulation cell, then each grain was randomly rotated around x in order to emulate the experimental regime of casual nucleation and columnar alignment along a preferential direction texturing. The system was finally thermally annealed at 1200K for as long as 3ns. The equations of motion were integrated through the velocity verlet algorithm with a time step of 1.0fs. Temperature was controlled by rescaling atomic velocities. The interatomic forces were calculated according to the environment dependent interatomic potential, consisting of two and three body angular terms which both depend on the local atomic co-ordination.

The computational tool used for study was

$$\theta(t, T) = \frac{1}{N} \left| \sum_l e^{ik \cdot r_l} \right|$$

Where r_l are the atomic co-ordinates at time t , $k = \frac{2\pi}{d}$, $0, O, l = 1, \dots, N$, was set parallel to the columnar x- oriented grains and d is interplanar distance along the [1,0,0] direction. The crystallinity of the sample was computed by

$$X(t) = \frac{\theta_{ac}(t, T) - \theta_a}{\theta_c(T) - \theta_a}$$

Where $\theta_c(T)$ and θ_a are the structure factors calculated at the reference temperature for bulk carbon silicon respectively. We calculated a constant $\theta_a \sim 0.1$ over all temperatures while $\theta_c(T)$ was calculated to decrease linearly with increasing temperature from $\theta_c = 1$ at $T = 0\text{ K}$ with $1 > \theta_c > \theta_a > 0$ for any $T > 0$ and below the carbon silicon melting temperature.

RESULTS AND DISCUSSION

We have calculated the velocity of amorphous crystalline boundaries in presence of hydrogen. We have used Kolmogorov Johnson-Mehl Avrami theory which related the time evolution of the overall crystallinity $X(t)$ to that of the individual volume gains $V(t)$. The regime of site saturation occurring when the nucleation time is small and the grains have similar size.

$$X(t) = X_{\infty} \left\{ 1 - e^{-\pi \rho [V(t+t_0)]^q} \right\}$$

Where $\rho = \frac{N}{L_x L_y}$ is the number of grains per area and $X_{\infty} \leq 1$ is the asymptotic

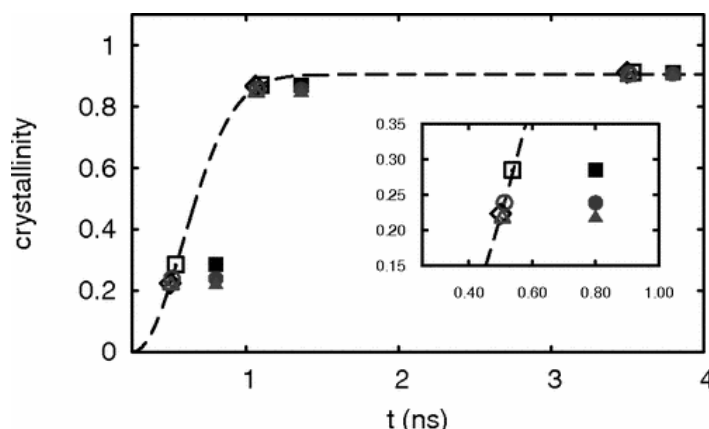
crystallinity. We used $N=20$. Graph (1) shows curve for $X(t)$ passing on the empty diamonds at points (0.5ns, 0.22), (1.06ns, 0.87) and (3.5ns, 0.91) corresponding to the initial non hydrogenated systems. The fitted parameters are $X_{\infty} = 0.905$, $q = 2.02$ and $v = 7.4$ m/s. The crystallinity of hydrogenated systems after the 0.3 ns long annealing correspond to filled symbols 0%, 3% and 6% correspond to squares, circles, triangles. The crystallinity increments ΔX_X^H upon annealing depend on both the sample crystallinity X and the hydrogen content H . Graph (1) shows a direct measurement of the velocity with respect to the reference environment dependent interatomic potential crystallization it was calculated from atomistic data

$$f^H = \frac{\Delta X_X^H}{\Delta t} / \frac{dx}{dt}(x)$$

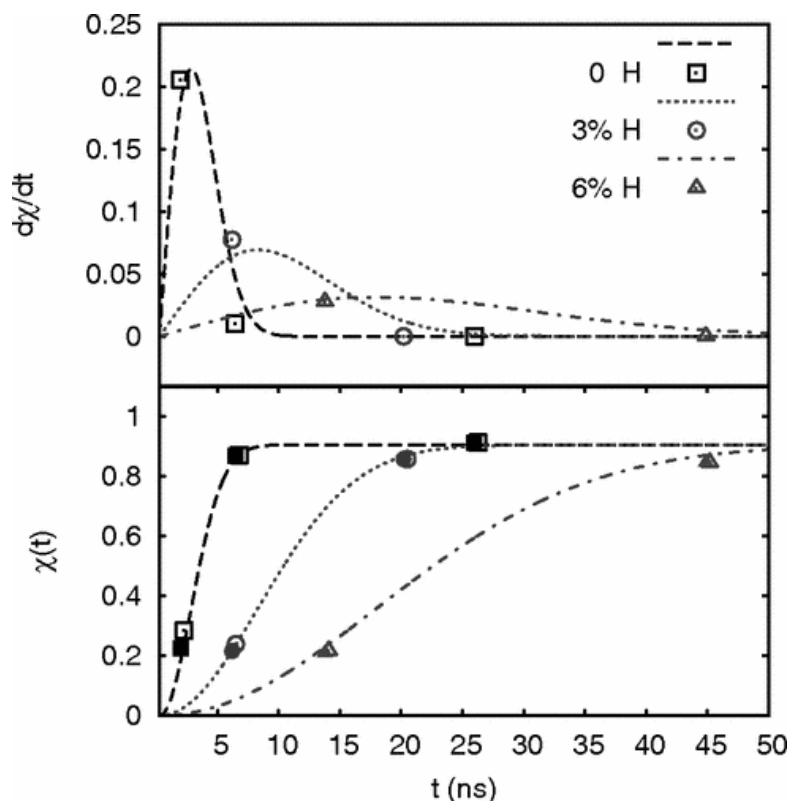
The crystallization kinetics calculated at 0%, 3%, and 6% H content is shown in graph (2) together

with the rate of recrystallization $\frac{dx}{dt}$. It was found that the crystallinity monotonically increased up to

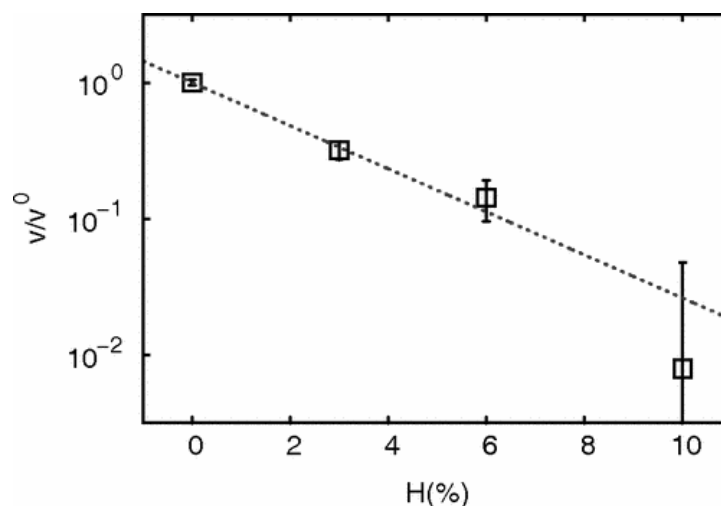
asymptotic limit X_{∞} , while the rate increased upto a maximum value and then decreased to zero at long annealing time when the systems were largely crystalline. By increasing the hydrogen content concentration for 0% to 6% the time scale for crystallization increased by almost one order of magnitude. Graph (3) shows the analysis of our result also, a-c boundary velocity v^H was shown as a function of hydrogen content velocities were normalized v^0 for which we obtained $v^0 = f^0 v^{ref} \sim 0.9$ m/s a value that is one order of magnitude smaller. We found that the formation of SiH aggregated impact on the microstructure evolution of nanocrystalline silicon. Hydrogen affected the recrystallization process by lowering the mobility of the a-c boundaries and characterized by the periodic pattern consisting of rectangular cells. The obtained results were compared with previously obtained results and were found in good agreement



Graph 1: Analytical model of crystallinity $\chi^{(t)}$ (dashed line corresponds to the pure silicon recrystallization) and atomistic data.



Graph 2: Crystallinity evolution $\chi(t)$ (bottom) and rate of recrystallization $\frac{d\chi}{dt}$ (top) of hydrogenated silicon simulated by the HV model for different hydrogen content.



Graph 3: Crystallization velocity as a function of hydrogen content.

CONCLUSION

We found that when hydrogen is dispersed in the film, it affects the relative stability between the amorphous and the crystalline phases and in turn the mobility of the phase boundaries during the solid phase crystallization of nanocrystalline -SiH . For medium high concentration, hydrogen was found to reduce the crystalline order of the system slowing down the crystallization. We found that

the recrystallization rate decreased exponentially with the hydrogen contamination. At low concentration the kinetic was moderately affected by the hydrogen atoms that tended to migrate to the boundaries increasing their effective interface. The obtained results were compared with previously obtained theoretical and experimental works and were found in good agreement.

REFERENCES

1. Vetterl. O, Finger. F, Carius. R, Hapke. P, Houben.L, Kluth.O, et al. (2000), Sol. Energy Mater. Sol Cells. 62, 97.
2. Spinella. C, Lombardo. S and Priolo. F., (1998), J. Appl. Phys. 84, 5383.
3. Cleri. F and Koblinski P., (2006), J. Comp. Sci. Eng. 2, 242.
4. Bergren M. R., Simonds. B.J., et al. (2013), Phys. Rev. B., 87, 081301.
5. Voyles. P.M. et al. (2001), Phys. Rev. Lett. 86, 5514.
6. Lucovsky. G., et al. (2011), Adv. Mat. 13, 1586.
7. Math. E., Naudon. A, (1992), Appl. Surf. Sci, 54, 392.
8. Tauc. J., Grigorivici. R. and Vancu. A, (1966), Phys. Status Solidi B, 15, 627.
9. Zhang. X. C.R. and Wu. H. (2009), Appl. Phys. Lett. 94, 242105.
10. Bagolini. L., et al. (2010), Phys. Rev. Lett. 104, 176803.
11. Godet. C, Layadi. N and Cabarrocas. P.R. (1995), Appl. Phys. Lett .66, 3146.
12. Sharma K., Verheijen M. A., Vande Sandan M.C. M. and Creatore. M. (2012), 111, 033508.